Supporting Information

Self-Supported Nickel Phosphosulphide Nanosheets for Highly Efficient and Stable Overall Water Splitting

Jie Luo[a,*], Haiyan Wang[a], Geng Su[a,*], Yuliang Tang[a], Huangqing Liu[b], Fenyang Tian[a], Deliang Li[a]

[a] School of Materials Science and Engineering, Central South University of Forestry and Technology, Changsha, Hunan 410004, PR China

[b] School of Physics and Electronics, Hunan University, Changsha，Hunan 410082, PR China

*Corresponding author. E-mail: clxy_luojie@csuft.edu.cn

sugeng1996@126.com

Supplementary results

Table S1. Elemental composition of Ni, P, and S in as-prepared and post-reaction $NiP_{0.62}S_{0.38}$, from ICP-AES and the corresponding BET surface area.

Electrodes	Composition (wt %)			Atomic ratio	BET (m^2/g)
	Ni	P	S	Ni:P:S	
$NiP_{0.62}S_{0.38}$ (fresh)	65.1	21.3	13.4	1:0.62:0.38	198
$NiP_{0.62}S_{0.38}$ (6 h after HER)	64.7	20.1	12.2	1:0.58:0.35	195
$NiP_{0.62}S_{0.38}$ (6 h after OER)	64.2	17.6	10.4	1:0.52:0.30	208

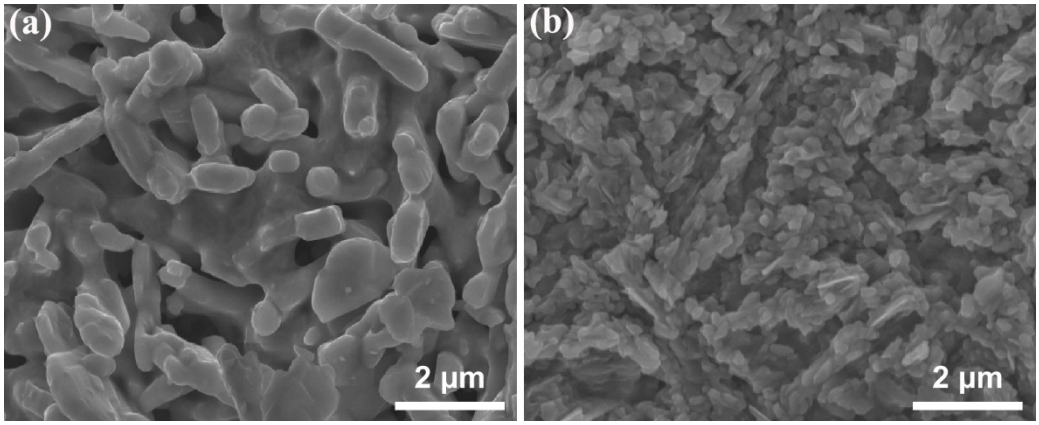

Fig. S1 Top-view SEM images of NiP and NiS.

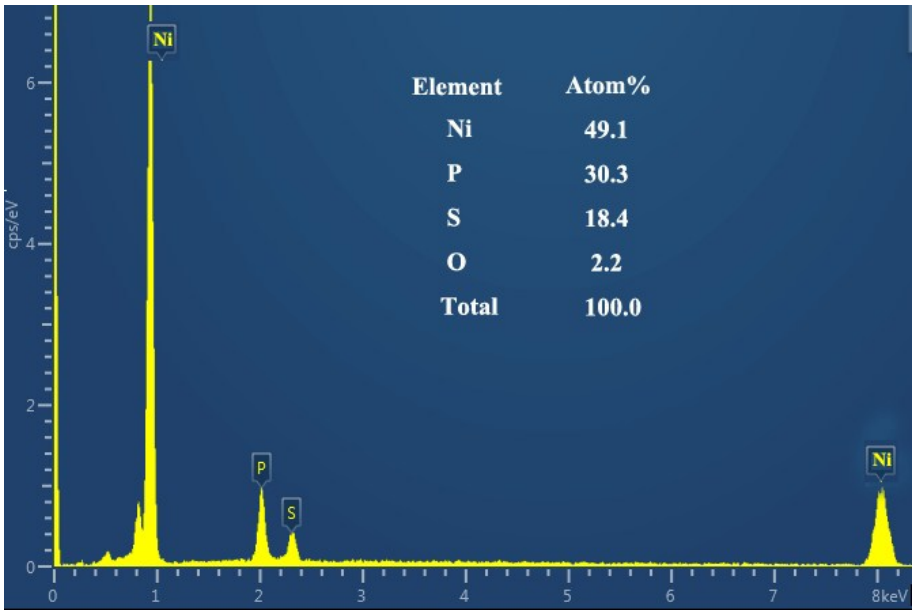

Fig. S2 EDS spectrum of $NiP_{0.62}S_{0.38}$ and the atomic ratio of corresponding elements.

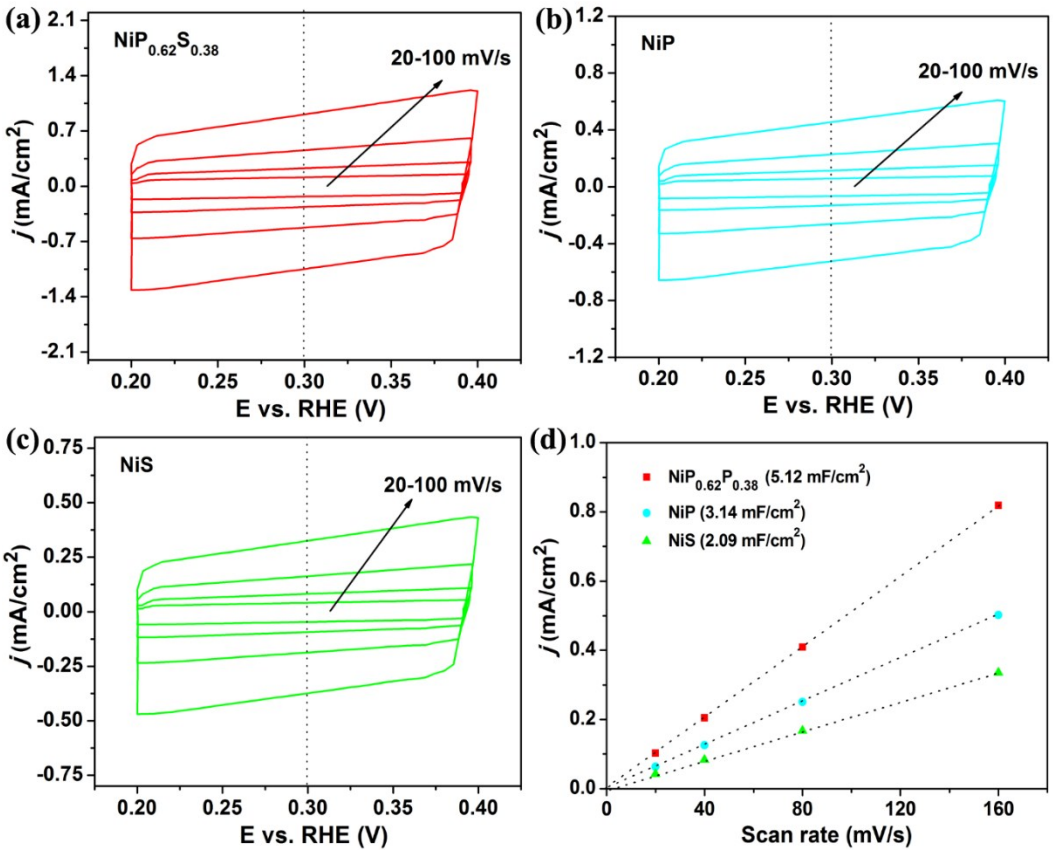

Fig. S3 Electrochemical capacitance measurements to determine the ECSA of the obtained electrodes in 1 M KOH for HER. The capacitive current density on (a) $NiP_{0.62}S_{0.38}$, (b) NiP, and (c) NiS can be measured from cyclic voltammograms in a potential range of 0.2-0.4 V vs. RHE where no Faradic reaction occur. (d) The measured capacitive current plotted as a function of scan rate.

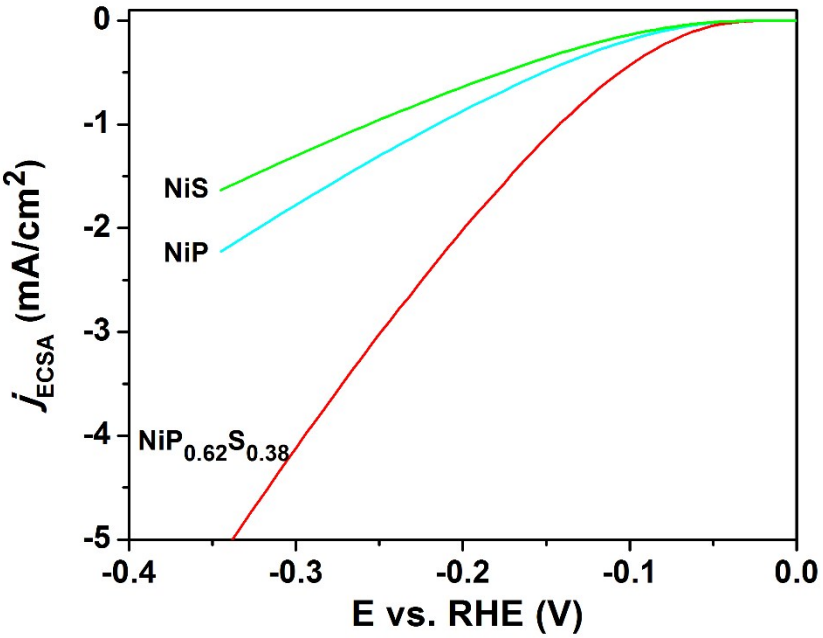

Fig. S4 Polarization curves with current density normalized by ECSA for $NiP_{0.62}S_{0.38}$, NiP and NiS.

Electrochemical active surface area and TOF calculation

Electrochemical capacitance measurements were used to determine the active surface area of the obtained catalysts, which is similar to the previous report [1]. The applied potential was kept between 0.2 to 0.4 V vs. RHE for four cycles at different scan rates (20, 40, 80, and 160 mV/s). The capacitive currents were measured in a potential range where no faradic reactions occurring and then obtain the current data at the middle potential value (0.3 V vs. RHE). Fig. S2c shows the measured capacitive currents were plotted as a function of scan rate, and the specific capacitance are determined to be about 5.12, 3.14, and 2.09 μF/cm^2 for $NiP_{0.62}S_{0.38}$, NiP, and NiS, respectively. In general, the specific capacitance for a flat surface is found to be in the range of 20-60 μF/cm^2, and we adopt the middle value of 40 μF/cm^2 to calculate the turnover frequency (TOF).

$$A_{\mathrm{ECSA}\ (NiP_{0.62}S_{0.38})} = \frac{\text{Total specific capacitance of } NiP_{0.62}S_{0.38}}{\text{specific capacitance of per real surface area}} = \frac{5.12\ mF/cm^2}{40\ \mu F/cm^2\ per\ ECSA\ cm^2} = 128.0\ cm^2_{ECSA}$$

$$A_{\mathrm{ECSA}\ (NiP)} = \frac{\text{Total specific capacitance } of\ NiP}{\text{specific capacitance of per real surface area}} = \frac{3.14\ mF/cm^2}{40\ \mu F/cm^2\ per\ ECSA\ cm^2} = 78.5\ cm^2_{EASA}$$

$$A_{\text{ECSA }(NiS)} = \frac{\text{Total specific capacitance } of\ NiS}{\text{specific capacitance of per real surface area}} = \frac{2.09\ mF/cm^2}{40\ \mu F/cm^2\ per\ ECSA\ cm^2} = 52.3\ cm^2_{EASA}$$

$$n_{H_2} = \left(j\frac{mA}{cm^2}\right)\left(\frac{1C \cdot S^{-1}}{1000\ mA}\right)\left(\frac{1\ mol\ e^-}{96485.3\ C}\right)\left(\frac{1\ mol\ H_2}{2\ mol\ e^-}\right)\left(\frac{6.022 \times 10^{23} H_2\ molecules}{1\ mol\ H_2}\right) = 3.12 \times 10^{15}\frac{H_2/s}{cm^2} per\ \frac{mA}{cm^2}$$

We consercatively estimate the number of active sites as the total number of surface sites (including both the nickel, phopshide, and sulfide atoms) because the exact hydrogen binding sites are not known. The volume of each cell for $NiP_{0.62}S_{0.38}$, NiP, and NiS is 89.88, 89.67 and 54.83 Å^3, respectively, thus

$$n^{surface\ sites}_{NiP_{0.62}S_{0.38}} = \left(\frac{16\ atoms\ per\ unit\ cell}{89.88\ Å^3\ per\ unit\ cell}\right)^{\frac{2}{3}} = 3.164 \times 10^{15} atoms\ per\ real\ cm^2$$

$$n^{surface\ sites}_{NiP} = \left(\frac{16\ atoms\ per\ unit\ cell}{89.67\ Å^3\ per\ unit\ cell}\right)^{\frac{2}{3}} = 3.168 \times 10^{15} atoms\ per\ real\ cm^2$$

$$n^{surface\ sites}_{NiS} = \left(\frac{4\ atoms\ per\ unit\ cell}{54.83\ Å^3\ per\ unit\ cell}\right)^{\frac{2}{3}} = 1.746 \times 10^{15} atoms\ per\ real\ cm^2$$

Finally, plot of current density can be converted into a TOF plot according to:

$$TOF_{NiP_{0.62}S_{0.38}} = \frac{(3.12 \times 10^{15}\frac{H_2/s}{cm^2} per \frac{mA}{cm^2}) \times |j_{NiP_{0.62}S_{0.38}}|}{n^{surface\ sites}_{NiP_{0.62}S_{0.38}} \times A_{ECSA\ (NiP_{0.62}S_{0.38})}} = 0.0077 \times |j_{NiP_{0.62}S_{0.38}}|$$

$$TOF_{NiP} = \frac{(3.12 \times 10^{15}\frac{H_2/s}{cm^2} per \frac{mA}{cm^2}) \times |j_{NiP}|}{n^{surface\ sites}_{NiP} \times A_{ECSA\ (NiP)}} = 0.0125 \times |j_{NiP}|$$

$$TOF_{NiS} = \frac{(3.12 \times 10^{15}\frac{H_2/s}{cm^2} per \frac{mA}{cm^2}) \times |j_{NiS}|}{n^{surface\ sites}_{NiS} \times A_{ECSA\ (NiS)}} = 0.0341 \times |j_{NiS}$$

Theoretical computation of free-energy for the HER

All calculations in this study were carried out using the Vienna ab initio simulation package (VASP) [2-4]. We used the PBE functional for the exchangecorrelation energy and projector augmented wave (PAW) potentials [5-7]. The kinetic energy cutoff was set to 450

eV. The ionic relaxation was performed until the force on each atom is less than 0.01 eV/Å. The k-points meshes were sampled based on the Monkhorst-Pack method [8]. DFT-D method was used to calculate the adsorption energy, which is an efficient method to approximately account for the long-range vdW interactions [9]. To minimize the undesired interactions between images, a vacuum of at least 15 Å was considered along the z-axis. DFT simulations were based on the experimentally crystal structure of NiP (ICDD: 01-074-1382) and NiS (ICDD: 01-075-0613). The structure of $NiP_{0.62}S_{0.38}$ and $NiP_{0.45}S_{0.55}$ were obtained by substituting phosphide atom within the unit cell with S atoms in all possible geometrics and selected the most stable ones. Chemisorption was modeled on the NiP, NiS, $NiP_{0.62}S_{0.38}$, and $NiP_{0.45}S_{0.55}$ (122) surfaces. The surfaces were constructed as slab consists of three layers within periodic boundary conditions, separated by a 20 Å vacuum layer. For these calculations, three layers with 2×2×1 k-point mesh was used in the 2×2 super cells for NiP, NiS, $NiP_{0.62}S_{0.38}$, and $NiP_{0.45}S_{0.55}$.

The HER activity on a specific system can be reflected by the adsorption energy of a single H atom on active sites of the system. The smaller ΔG_{H^*} absolute value means the better activity on the HER catalysts. The adsorption free energy was calculated by

$$\Delta G_H = \Delta E_H + \Delta E_{ZPE} - T\Delta S_H$$

where ΔE_{ZPE} and ΔS_H are the differences in zero point energy and entropy between the H adsorbed state and H_2 in its gas phase. The hydrogen binding energies were calculated by

$$\Delta E_H = E(surf + H) - E(surf) - \frac{1}{2}E(H_2)$$

where E(surf + H), E(surf) and $E(H_2)$ are the total energies of the surfaces with 1 hydrogen atom adsorbed, the pristine surfaces and gas phase hydrogen molecular respectively.

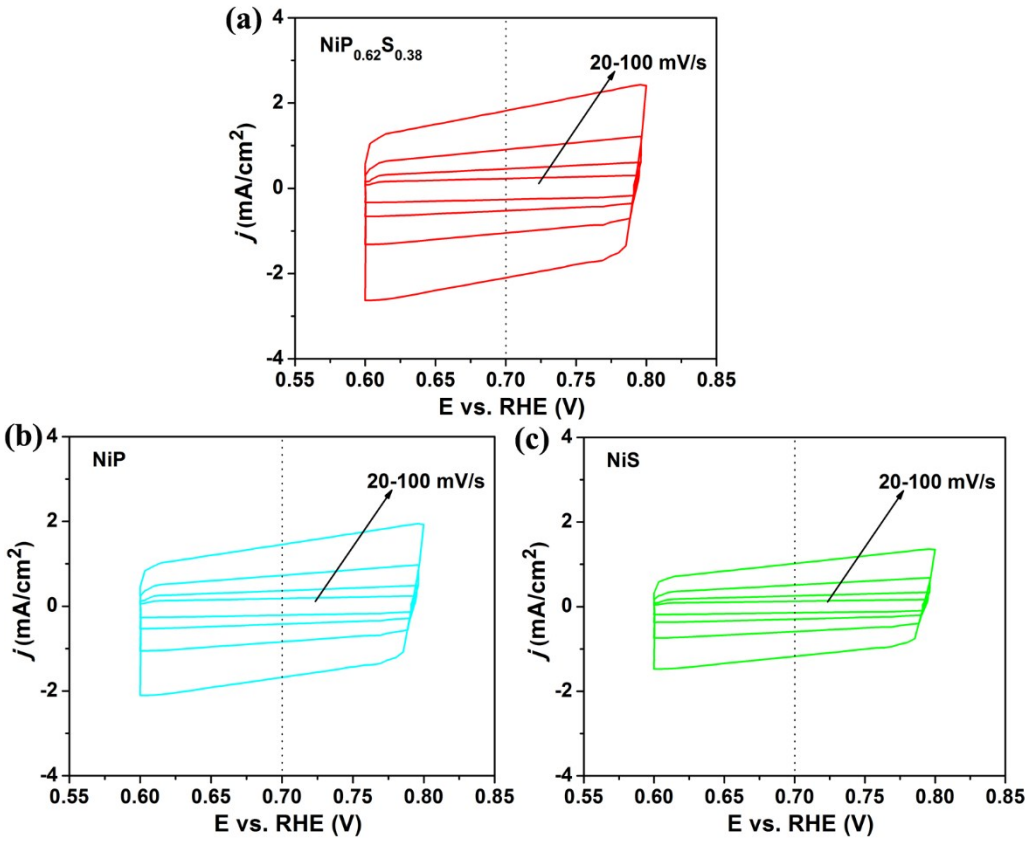

Fig. S5 Electrochemical capacitance measurements to determine the ECSA of the obtained electrodes in 1 M KOH for OER. The capacitive current density on (a) $NiP_{0.62}S_{0.38}$, (b) NiP, and (c) NiS can be measured from cyclic voltammograms in a potential range of 0.6-0.8 V vs. RHE where no Faradic reaction occur.

Table S2 Comparison of HER activity in alkaline electrolyte (1 M KOH) for $NiP_{0.62}S_{0.38}$ with other recently reported highly active HER electrocatalysts.

Catalyst	η_{10} (mV)	η_{20} (mV)	*Tafel slope (mV/dec)*	Ref.
$NiP_{0.62}S_{0.38}$	52	70	52.3	*This Work*
$Ni_{0.51}Co_{0.49}P$	82		50.4	*Adv. Funct. Mater. 2016,26,7644*
Ni_5P_4	150		53	*Angew.Chem.Int.Ed.2015,54,12361*
CP@Ni-P	117	150	85.4	*Adv.Funct.Mater. 2016,26,4067*
Co-P film	94	115	42	*Angew.Chem.Int.Ed. 2015,54,6251.*
$Ni_{1-x}Co_xP$	82		43	*Adv. Funct. Mater. 2016,26,7644.*
$NiCo_2O_4$	110		49.7	*Angew.Chem.Int.Ed. 2016,55,6290.*
CoFePO	87.5		38.1	*ACS Nano 2016,10,8738.*
NiCoFe LDHs	200		70	*ACS Energy Lett. 2016,1,445.*
Ni_3S_2/NF	223			*J. Am.Chem.Soc.2015,137,14023.*
MoS_2/Ni_3S_2	110		83	*Angew.Chem.Int.Ed.2015,128,6814*
h-NiS_x	60	89	99	*Adv. Energy Mater.2016,6,1502333*
MoOx/Ni_3S_2/NF	106		90	*Adv. Funct. Mater.2016,26,4839.*
$NiCo_2S_4$ NWs/NF	210		58.9	*Adv.Funct.Mater.2016,26,4661.*

Table S3 Comparison of OER activity in alkaline electrolyte (1 M KOH) for $NiP_{0.62}S_{0.38}$ with other recently published highly active OER electrocatalysts

Catalyst	η_{10} **(mV)**	η_{20} **(mV)**	***Tafel slope (mV/dec)***	**Ref.**
$NiP_{0.62}S_{0.38}$	240	280	46	*This Work*
np-$(Co_{0.52}Fe_{0.48})_2P$	270		30	*Energy Environ.Sci.2016,9,2257*
NiCoP	280		85	*Nano Lett.2016,16,7718*
Co-P film	345		47	*Angew.Chem.Int.Ed. 2015,54,6251*
Ni_2P	290		47	*Energy Environ. Sci. 2015,8,2347*
Co/CoP-5	340		79.5	*Adv.EnergyMater.2017,10.1002/aenm.201602355*
CP/CTs/Co-S	306		72	*ACS Nano 2016,10,2342*
Ni_3Se_2-GC	310		79.5	*Energy Environ. Sci. 2016, 9, 1771*
$Mn_3O_4/CoSe_2$	450		49	*J.Am.Chem.Soc.2012,134,2930*
NiD-PCC	360		98	*Energy Environ. Sci. 2016, 9, 3411*
ONPPG/OCC	410		83	*Energy Environ. Sci. 2016, 9, 1210*
NG-CoO	340		65	*Energy Environ. Sci. 2014, 7, 609*
$Zn_xCo_{3-x}O_4$ NWs	320		51	*Chem.Mater.2014,26,1889*
CoCo LDH	380		59	*Nat.Commun.2014,5,4477*
Co_3O_4/NG	310		67	*Nat.Mater.2011,10,780*
CoMn LDH	320		43	*J.Am.Chem.Soc.2014,136,16481*

Table S4 Summary of overall alkaline water splitting performance of recently reported highly efficient bifunctional non-noble electrocatalysts.

Catalyst	$E_{j=10}$ (mV)	Ref.
$NiP_{0.62}S_{0.38}$||$NiP_{0.62}S_{0.38}$	1.52	*This Work*
$(Co_{0.52}Fe_{0.48})_2P$||$(Co_{0.52}Fe_{0.48})_2P$	1.53	*Adv. Energy Mater.2016,6,1502313*
NiCoP||NiCoP	1.58	*Nano Lett.2016,16,7718*
$Ni_{0.51}Co_{0.49}P$/ $Ni_{0.51}Co_{0.49}P$	1.57	*Adv. Funct. Mater. 2016,26,7644.*
Ni_2P-NF/Ni_2P-NF	1.63	*Energy Environ. Sci. 2015,8,1027*
CoP-Cu/CoP-Cu	1.645	*Angew.Chem.Int.Ed.2015,54,6251*
$Ni_{12}P_5$-NF/ $Ni_{12}P_5$-NF	1.64	*ACS Catal.2015,7.103.*
CP@Ni-P/CP@Ni-P	1.63	*Adv.Funct.Mater. 2016,26,4067*
Ni_5P_4/ Ni_5P_4	1.7	*Angew.Chem.Int.Ed.2015,54,12361.*
NiCoP-NF/NiCoP-NF	1.58	*Nano Lett. 2016,16,7718*
CoP-MNA/CoP-MNA	1.62	*Adv.Funct.Mater.2015,25,7337*
$NiCo_2S_4$-NF/ $NiCo_2S_4$-NF	1.63	*Adv.Funct.Mater.2016,26,4661.*
$CoSe_2$-CC/$CoSe_2$-CC	1.63	*Adv. Mater.2016,28,7527*
NiSe-NF/NiSe-NF	1.63	*Angew.Chem.Int.Ed.2015,54,9351*
CP-CTs-Co-S/ CP-CTs-Co-S	1.74	*ACS. Nano 2016, 10, 2342*
FeCoNi-CC/FeCoNi-CC	1.66	*ACS Catal.2017,7,469*
VOOH/VOOH	1.62	*Angew.Chem.Int.Ed.2017,129,588*
$NiCo_2O_4$/$NiCo_2O_4$	1.65	*Angew.Chem.Int.Ed. 2016,55,6290*
NiFe LDH-NF/ NiFe LDH-NF	1.70	*Science 2014, 345,1593*

Reference

[1] J. Kibsgaard, C. Tsai, K. Chan, J. D. Benck, J. K. Norskov, F. Abild-Pedersen, T. F. Jaramillo, Energy Environ. Sci. 8 (2015) 3022-3029.

[2] G. Kresse, J. Furthmuller, Comp. Mater. Sci. 6 (1996) 15-50.

[3] G. Kresse, J. Furthmuller, Phys. Rev. B 54 (1996) 11169-11186.

[4] G. Kresse, J. Hafner, Phys. Rev. B 49 (1994) 14251-14269.

[5] J. P. Perdew, K. Burke, M. Ernzerhof, Phys. Rev. Lett. 78 (1997) 1396.

[6] G. Kresse, D. Joubert, Phys. Rev. B 59 (1999) 1758-1775.

[7] P. E. Blochl, Phys. Rev. B 50 (1994) 17953-17979.

[8] H. J. Monkhorst, J. D. Pack, Phys. Rev. B 13 (1976) 5188-5192.

[9] S. J. Grimme, Comput. Chem. 27 (2006) 1787-1799.